Proc. Natl. Acad. Sci. USA
Vol. 76, No. 5, pp. 2109–2113, May 1979
Physics

Numerical analysis of weakly nonlinear wave turbulence

(Hamilton's principle/wave–wave interactions/oceanic internal waves/relaxation phenomena/statistical mechanics)

JAMES D. MEISS, NEIL POMPHREY, AND KENNETH M. WATSON

Department of Physics and Lawrence Berkeley Laboratory, University of California, Berkeley, California 94720

Contributed by Kenneth M. Watson, January 29, 1979

ABSTRACT **We consider the propagation of weakly nonlinear waves such as plasma waves, surface water waves, the interaction of laser beams with matter, particle accelerators, etc. Specifically, we study internal waves in the ocean. Hamilton's principle is used to write the fluid equations in Hamiltonian form in terms of linear eigenmode amplitudes. Numerical studies are made of the effect of Fourier grid size and resonance widths. Statistical information is generated from an ensemble of initial states of the random wave field.**

1. Introduction

In this paper we study the statistical properties of weak turbulence associated with nonlinear wave–wave interactions. Specifically, we apply the analysis to buoyancy-dominated turbulence of internal waves in the ocean. Stable stratification, a characteristic of the oceans, implies an equilibrium depth about which each fluid element oscillates. The resulting "almost two-dimensional" system avoids some of the complexity of fully three-dimensional weak turbulence.

Formally, our wave system corresponds to a set of harmonic oscillators with weakly nonlinear couplings. Similar dynamical systems are encountered in the study of surface water waves (1), plasma waves (2), the interaction of light with matter, particle accelerators, and other branches of physics (3).

Weakly nonlinear oscillator systems have been studied by several statistical models. Use of *random phase* and two-time scale approximations allows termination of a sequence of coupled moment equations to give a Boltzmann-type transport equation (4–6). In a future publication we will show how the fluctuation-dissipation theorem and the Krylov–Bogoliubov–Mitropolsky (KBM) perturbation method can be used to obtain Langevin and Fokker–Planck equations.

These models can be compared with numerical solutions of the equations of motion, providing evidence for the validity of the approximations used. The ocean internal wave system lends itself particularly well to numerical computation because of the almost two-dimensional nature of the equations. Recently, the Hasselmann transport theory (4) has been applied to this system by McComas and Bretherton (7) and Olbers (8).

We derive an explicit Hamiltonian to describe the nonlinear transfer of energy among the linear eigenmodes of the internal wave field. A "test wave" model is developed, which can be used to compare numerical results with statistical models. This model describes the propagation of a single labeled wave through an ambient medium. Computational methods for integration of Hamilton's equations are also discussed.

2. Dynamical formulation of the wave interactions

We consider as a model a "plane" ocean of uniform depth and having rectangular area Σ_0. Periodic boundary conditions are used at the sides, and the top ($z = 0$) and bottom ($z = -H$) surfaces are assumed rigid. The equilibrium fluid density is $\rho(z)$, a monotonically increasing function of depth. The quantity

$$N(z) = \left[-\frac{g}{\rho}\frac{d\rho}{dz}\right]^{1/2} \qquad [2.1]$$

is the Väisälä, or buoyancy frequency (g is the acceleration due to gravity). The fluid is incompressible and inviscid.

We introduce a Lagrangian and use Hamilton's principle to obtain the equations of fluid motion. The Lagrange coordinate of a fluid particle at time t is $\mathbf{Y}(\mathbf{r},t)$, in which $\mathbf{r} = \mathbf{Y}(\mathbf{r},0)$ is its position at $t = 0$. The appropriate Lagrangian per unit area is

$$L = \int \frac{d^3r}{\Sigma_0}\left(\tfrac{1}{2}\rho|\dot{\mathbf{Y}}|^2 + \rho\mathbf{g}\cdot\mathbf{Y} - \tfrac{1}{2}\rho\mathbf{f}\cdot(\dot{\mathbf{Y}}\times\mathbf{Y}) + P(\mathbf{r})\left[J\left(\frac{\partial\mathbf{Y}}{\partial\mathbf{r}}\right) - 1\right]\right). \qquad [2.2]$$

[This Lagrangian is discussed by Bretherton and Garrett (9). McComas and Bretherton (7) use Lagrange's equations for their discussion.] The first three terms in the integrand represent, respectively, kinetic energy, negative of gravitational potential energy, and rotational energy due to Coriolis coupling. The quantity $\mathbf{f}$ is twice the angular frequency of the earth's rotation. The final term expresses the constraint due to incompressibility: P is a Lagrange multiplier and J is the Jacobian of the transformation $\mathbf{r} \rightarrow \mathbf{Y}$.

Hamilton's principle states that the functional

$$I = \int_{t_1}^{t_2} L\,dt \qquad [2.3]$$

is stationary with respect to arbitrary independent variations in $\mathbf{Y}$ and P, which vanish at t_1 and t_2 and at the boundaries of the fluid. In particular, variation of P yields the incompressibility condition

$$J\left(\frac{\partial\mathbf{Y}}{\partial\mathbf{r}}\right) = 1, \qquad [2.4]$$

and variation of $\mathbf{Y}$ yields the equations of motion

$$\rho\ddot{\mathbf{Y}} - \rho\mathbf{g} + \rho\mathbf{f}\times\dot{\mathbf{Y}} + \frac{\partial}{\partial\mathbf{Y}}P = 0. \qquad [2.5]$$

The Lagrange multiplier P can therefore be identified with the fluid pressure. It may be considered a function of $\mathbf{Y}$ and t in the Lagrangian because this adds terms with zero variation.

Rather than use Eqs. **2.4** and **2.5** directly, we develop a perturbation-variation approach with the aim of obtaining a Hamiltonian that describes the lowest-order nonlinear internal wave motions. Following Bretherton and Garrett (9), we define the displacement

$$\xi(\mathbf{r},t) \equiv \mathbf{Y}(\mathbf{r},t) - \mathbf{r}, \qquad [2.6]$$

and consider $|\xi|$ to be a *small* quantity. Expanding $P(\mathbf{Y},t)$,

The publication costs of this article were defrayed in part by page charge payment. This article must therefore be hereby marked "*advertisement*" in accordance with 18 U. S. C. §1734 solely to indicate this fact.

Abbreviation: KBM, Krylov–Bogoliubov–Mitropolsky.

substituting into Eqs. **2.2**, and omitting terms independent of ξ yields

$$L = \int \frac{d^3r}{\Sigma_0} [\tfrac{1}{2}\rho|\dot{\xi}|^2 + \rho \mathbf{g}\cdot\xi - \tfrac{1}{2}\rho \mathbf{f}\cdot(\dot{\xi}\times\xi) - (\xi\cdot\nabla)P(\mathbf{r},t) - \tfrac{1}{2}(\xi_i\xi_j\nabla_i\nabla_j)P(\mathbf{r},t) + \dots]. \quad [2.7]$$

Next, we define the pressure fluctuation

$$\pi(\mathbf{r},t) \equiv P(\mathbf{r},t) - P(\mathbf{r}) \quad [2.8]$$

and assume it is a small quantity of the same order as $|\xi|$. Using definition **2.8** in Eq. **2.7**, we obtain

$$L = L_1 + L_2 + L_3 + \dots,$$

$$L_1 = \int \frac{d^3r}{\Sigma_0} [\rho \mathbf{g}\cdot\xi - (\xi\cdot\nabla)P(\mathbf{r})],$$

$$L_2 = \int \frac{d^3r}{\Sigma_0} \left[\tfrac{1}{2}\rho|\dot{\xi}|^2 - \frac{\rho}{2}\mathbf{f}\cdot(\dot{\xi}\times\xi) - (\xi\cdot\nabla)\pi - \tfrac{1}{2}(\xi_i\xi_j\nabla_i\nabla_j)P(\mathbf{r})\right],$$

$$L_3 = \int \frac{d^3r}{\Sigma_0} [-\tfrac{1}{2}(\xi_i\xi_j\nabla_i\nabla_j)\pi - \tfrac{1}{6}(\xi_i\xi_j\xi_k\nabla_i\nabla_j\nabla_k)P(\mathbf{r})]. \quad [2.9]$$

The equations of motion in each order are obtained by variation of the action with respect to ξ and π. Variation of I_1 with respect to ξ identifies $P(\mathbf{r})$ as the hydrostatic pressure, $\nabla_3 P = -\rho g$. Subsequent elimination of P from the Lagrangian allows us to ignore I_1 from now on.

The linear equations of motion are obtained by variation of I_2:

$$\rho\ddot{\xi} + \rho \mathbf{f}\times\dot{\xi} + \nabla\pi + \rho N^2\xi_3\hat{z} = 0,$$

$$\nabla\cdot\xi = 0, \quad [2.10]$$

in which N^2 is defined by Eq. **2.1**.

We now neglect the horizontal components of $\mathbf{f}$ (see, for example, ref. 1, p. 239). This enables us to separate the horizontal and vertical parts of Eq. **2.10** and expand $\xi_3(\mathbf{x},z,t)$ in the rectangular area Σ_0 as†

$$\xi_3(\mathbf{x},z,t) = \sum_{\alpha=1}^{\infty}\sum_{\mathbf{k}} A_{\mathbf{k}\alpha}(t)W_{k\alpha}(z)e^{i\mathbf{k}\cdot\mathbf{x}}$$

$$A_{-\mathbf{k}\alpha} = A^*_{\mathbf{k}\alpha} \quad [2.11]$$

(the first sum extends over all positive integers α). Our task will be to obtain an expression for the Lagrangian **2.9** in terms of the field amplitudes $A_{\mathbf{k}\alpha}(t)$.

Straightforward algebra yields

$$\nabla_3\rho\nabla_3 W_{k\alpha} + \rho k^2\left(\frac{N^2-\omega_\alpha^2(k)}{\omega_\alpha^2(k)-f^2}\right)W_{k\alpha} = 0,$$

$$\omega_\alpha(k) > 0,$$

$$W_{k\alpha}(-H) = W_{k\alpha}(0) = 0. \quad [2.12]$$

This is a Sturm–Liouville equation for the modefunctions $W_{k\alpha}(z)$ and eigenvalues $\omega_\alpha(k)$. The orthogonality relations

$$\frac{1}{\rho_0}\int_{-H}^{0}\rho[N^2(z)-f^2]W_{k\alpha}W_{k\beta}dz = \delta_{\alpha\beta} \quad [2.13]$$

are readily deduced from Eq. **2.12**. The quantity ρ_0 may, for example, be chosen as $\rho(0)$. The Fourier amplitudes $A_{\mathbf{k}\alpha}$ satisfy the equation

$$\ddot{A}_{\mathbf{k}\alpha} + \omega_\alpha^2(k)A_{\mathbf{k}\alpha} = 0. \quad [2.14]$$

† Henceforth all vectors with the exception of $\mathbf{f}$ will be two-dimensional in the horizontal plane.

The horizontal displacement ξ_h is expressed in the form

$$\xi_h(\mathbf{x},z,t) = \sum_{\alpha=1}^{\infty}\sum_{\mathbf{k}} [i\mathbf{k}A_{\mathbf{k}\alpha} + (i\mathbf{k}\times\mathbf{f})B_{\mathbf{k}\alpha}]\frac{1}{k^2}W'_{k\alpha}e^{i\mathbf{k}\cdot\mathbf{x}}, \quad [2.15]$$

in which $\dot{B}_{\mathbf{k}\alpha} = A_{\mathbf{k}\alpha}$ and $W' \equiv dW/dz$. The pressure fluctuation is then

$$\pi = -\rho\sum_{\alpha=1}^{\infty}\sum_{\mathbf{k}}(\ddot{A}_{\mathbf{k}\alpha} + f^2A_{\mathbf{k}\alpha})\frac{1}{k^2}W'_{k\alpha}e^{i\mathbf{k}\cdot\mathbf{x}}. \quad [2.16]$$

These expansions may be introduced into expression **2.9** for L_2 to give

$$L_2 = \frac{\rho_0}{2}\sum_{\alpha=1}^{\infty}\sum_{\mathbf{k}}\left[\frac{1}{\omega_\alpha^2(k)-f^2}(\dot{A}_{\mathbf{k}\alpha}\dot{A}_{-\mathbf{k}\alpha} - \omega_\alpha^2(k)A_{\mathbf{k}\alpha}A_{-\mathbf{k}\alpha})\right]. \quad [2.17]$$

The variational principle allows us to obtain L_2 and L_3 from the linear expressions **2.11–2.16.** In particular, we may use Eq. **2.14** to eliminate time derivative terms from L_3. It is important to realize that the nonlinear fields will continue to be expressed in the form **2.11–2.16** except that **2.14** will be modified.

To express our equations in Hamiltonian form we replace the Fourier amplitudes $A_{\mathbf{k}\alpha}$ by canonical action-angle variables (see ref. 10) $J_{\mathbf{k}\alpha}$, $\theta_{\mathbf{k}\alpha}$:

$$A_{\mathbf{k}\alpha} = \frac{i}{\sqrt{2\omega_\alpha e_{k\alpha}}}\left[\sqrt{J_{\mathbf{k}\alpha}}\,e^{-i\theta_{\mathbf{k}\alpha}} - \sqrt{J_{-\mathbf{k}\alpha}}\,e^{i\theta_{-\mathbf{k}\alpha}}\right]$$

$$e_{k\alpha} \equiv \frac{\rho_0}{\omega_\alpha^2 - f^2}. \quad [2.18]$$

The resulting Hamiltonian is obtained after straightforward but tedious effort:

$$H = H_2 + H_3,$$

$$H_2 = \sum_{\alpha,\mathbf{k}}\omega_\alpha(k)J_{\mathbf{k}\alpha},$$

$$H_3 = \sum_{k,l,m}(J_kJ_lJ_m)^{1/2}\{\delta_{\mathbf{k}-\mathbf{l}-\mathbf{m}}\Gamma_1(k;l,m)\times\exp[i(\theta_k-\theta_l-\theta_m)] + \delta_{\mathbf{k}+\mathbf{l}+\mathbf{m}}\Gamma_2(k,l,m)\exp[i(\theta_k+\theta_l+\theta_m)]\} + \text{complex conjugate.} \quad [2.19]$$

(The coefficients Γ_1 and Γ_2 are given in the *Appendix.*) To simplify notation in H_3 we have written k for the index pair $(\mathbf{k},\alpha)$, etc.

For linear waves, corresponding to neglect of H_3, we have

$$\dot{J}_{\mathbf{k}\alpha} = 0, \quad \dot{\theta}_{\mathbf{k}\alpha} = \omega_\alpha(k). \quad [2.20]$$

Because H_3 is assumed small compared with H_2, terms involving Γ_2 are rapidly oscillating on the time scale of energy transfer among the modes. We shall henceforth neglect these terms.

Another set of convenient variables are the dimensionless action-amplitude variables‡

$$a_{\mathbf{k}\alpha} = \frac{k}{N_0\sqrt{B}}\left(\frac{2J_{\mathbf{k}\alpha}}{e_{k\alpha}\omega_\alpha}\right)^{1/2}e^{-i\theta_{\mathbf{k}\alpha}}. \quad [2.21]$$

They are related to the original Fourier coefficients $A_{\mathbf{k}\alpha}$ by

$$A_{\mathbf{k}\alpha} = i\frac{N_0\sqrt{B}}{2k}[a_{\mathbf{k}\alpha} - a^*_{-\mathbf{k}\alpha}]. \quad [2.22]$$

‡ N_0 and B are constant quantities having dimensions of frequency and length, respectively. They may be considered as scale parameters of the Väisälä profile $N(z)$.

In the linear approximation, $a_{\mathbf{k}\alpha}$ represents the amplitude of a traveling plane wave having wave number $\mathbf{k}$ and mode number α. It is normalized to describe the wave slope amplitude.

The equations of motion in terms of the $a_{\mathbf{k}\alpha}$ are

$$\dot{a}_k + i\omega_\alpha a_k = \sum_{lm} [\delta_{\mathbf{k+l-m}} G^{kl}_m a^*_l a_m + \delta_{\mathbf{k-l-m}} G^k_{lm} a_l a_m]. \quad [2.23]$$

The coefficients G are expressed in the *Appendix* as functions of Γ_1.

3. Test wave model

To provide a simple model for preliminary study we introduce the *test wave* system. Here a single $(\mathbf{k},\alpha)$ mode, identified as the test wave, is permitted to interact with an ambient field consisting of the remaining modes. However, the ambient modes are not allowed to interact among themselves. Test wave models are often employed for calculating relaxation rates in transport theory, where standard approximation schemes in statistical mechanics may be applied. Numerical integration of the equations of motion can be used to evaluate the validity of these approximation methods.

Our system consists of $2M + 1$ waves formed in M triads. We let k designate the test wave mode $(\mathbf{k},\alpha)$ and l,m designate ambient wave pairs $(\mathbf{l},\beta)$, $(\mathbf{m},\gamma)$, respectively. The appropriate equations of motion are then

$$\text{Test wave:} \quad \dot{a}_k + i\omega_\alpha a_k = \sum_{lm} [\delta_{\mathbf{k-l-m}} G^k_{lm} a_l a_m + \delta_{\mathbf{k+l-m}} G^{kl}_m a^*_l a_m].$$

$$\text{Background:} \quad \dot{a}_l + i\omega_\beta a_l = \delta_{\mathbf{l-k-m}} 2G^l_{km} a_k a_m + \delta_{\mathbf{l-k+m}} G^{lm}_k a_k a^*_m + \delta_{\mathbf{l+k-m}} G^{lk}_m a^*_k a_m. \quad [3.1]$$

It is easily verified that Eqs. **3.1** admit $M + 1$ conservation laws (see ref. 10).

In our computations, initial conditions for the ambient modes are chosen from a Gaussian distribution for the action-amplitudes. The initial wave phases are chosen from a distribution uniform in $-\pi,\pi$. Averages over ambient initial conditions will be denoted $\langle\,\rangle$. The mean square action amplitude, $\sigma_{\mathbf{k}\alpha}$, is related to the power density spectrum for the vertical displacement

$$\langle \xi^2_3 \rangle = \sum_{\alpha=1}^{\infty} \int d^2k \psi(\mathbf{k},\alpha); \quad [3.2]$$

$$\langle |a_{\mathbf{k}\alpha}|^2 \rangle = \sigma_{\mathbf{k}\alpha} = 2k^2 \left(\frac{4\pi^2}{\Sigma_0}\right) \psi(\mathbf{k},\alpha). \quad [3.3]$$

The specific $\psi(\mathbf{k},\alpha)$ for this study was the Garrett–Munk "75+" spectrum (11), an experimentally derived spectrum for internal waves that appears to be an equilibrium spectrum for the ocean.

4. Numerical methods and results

Our emphasis in this section will be on computational techniques and *qualitative* features of solutions. Detailed application to the ocean will be published separately.

For an ocean with square area Σ_0, the wave numbers form a grid with spacing

$$\Delta k_x = \Delta k_y = \frac{2\pi}{\sqrt{\Sigma_0}}. \quad [4.1]$$

Because the test-wave wave number $\mathbf{k}$ is fixed (given), the wave number conservation equations, $\mathbf{k} = \mathbf{m} \pm \mathbf{l}$, imply that a single grid can act as coordinate system. For example, choosing the x axis along $\mathbf{k}$, each point (m_x,m_y) defines a triad. The most important triads for energy transfer are expected to be those for which the "resonance conditions" $\Delta \equiv \omega_\alpha \mp \omega_\beta - \omega_\gamma \simeq 0$ hold. For a given set of modenumbers α,β,γ and a given resonance mismatch Δ, each resonance condition defines a curve in the m_x,m_y plane. Our procedure will be to include those triads that lie on grid points for which $|\Delta| \leq \Delta_{\max}$. For a given computation the parameters Δk and $\Delta_{\max}$ must be obtained empirically. Before discussing this further we present a sample computation of the full system of equations to illustrate the general character of the solution.

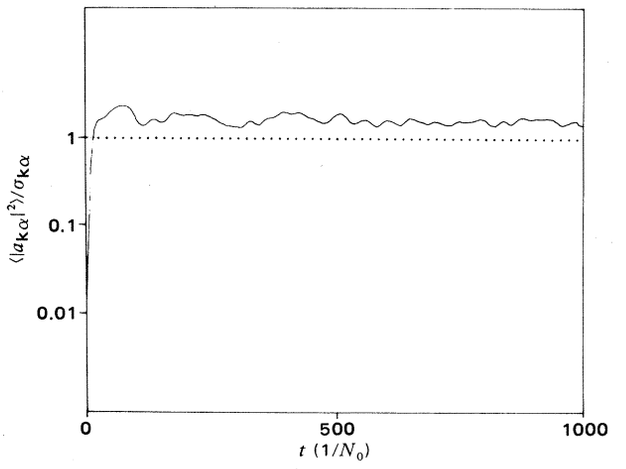

FIG. 1. Mean test wave action as a function of time with 91 triads on 15 resonance curves and coupling coefficients for the deep ocean. $\alpha = 4$, $\omega_\alpha = 7f$, and the mean is taken over $I = 100$ initial conditions.

Fig. 1 displays a typical example of the mean test wave action for the ocean internal wave system. The frequency and modenumber of the test wave are $\omega_\alpha = 7f$ and $\alpha = 4$, respectively. We include the first nine WKB (Wentzel–Kramers–Brillouin) vertical modes of the ambient spectrum. This corresponds to including 15 resonance curves in the calculation. The magnitude of the initial test wave action-amplitude is chosen to be 0.1 $\sqrt{\sigma_{\mathbf{k}\alpha}}$ and the corresponding initial phase is fixed arbitrarily. The ambient initial conditions are picked from the prescribed distribution with a random number generator. The test wave action is averaged over $I = 100$ ambient realizations, integrating Eqs. **3.1** to $t = 1000/N_0$ for each. The entire computation required approximately 7 min central processer time on a CDC 7600 computer. The salient features of Fig. 1 are a rapid rise of the test wave action by a factor of 100 in the first 20 time units, followed by small oscillations about a value slightly larger than its expected (Garrett–Munk) equilibrium value (indicated by the dashed horizontal line). We have found that these fluctuations decrease with increasing I, and that the mean value is constant upon variation of the initial test wave amplitude, providing this amplitude is small ($\leq 0.25\sqrt{\sigma_{\mathbf{k}\alpha}}$).

The effect of choosing different values of Δk and $\Delta_{\max}$ is best illustrated by a simple model calculation. For the remainder of this section we keep only those interactions in Eqs. **3.1** with $\mathbf{k} = \mathbf{l} + \mathbf{m}$ and arbitrarily set the coupling coefficients to $G^k_{lm} = G^{lm*}_k = G^{ml*}_k = G \equiv \frac{1}{2}(-1 + i)$, ignoring the complicated wave number and frequency dependence of the real ocean.

To investigate the effect of off-resonant triads, we consider 25 triads, 13 with $\Delta = 0$ and 12 with $\Delta = \Delta_{\max}$. Fig. 2 presents the short-time behavior of the mean action for various $\Delta_{\max}$. For the dotted curves the phases of the ambient modes at $t = 0$ are chosen so that the initial growth rate of the test wave action is maximal (the sum of the phases of the background waves in Eqs. **3.1** plus the phase of G is zero). It is known that this set of

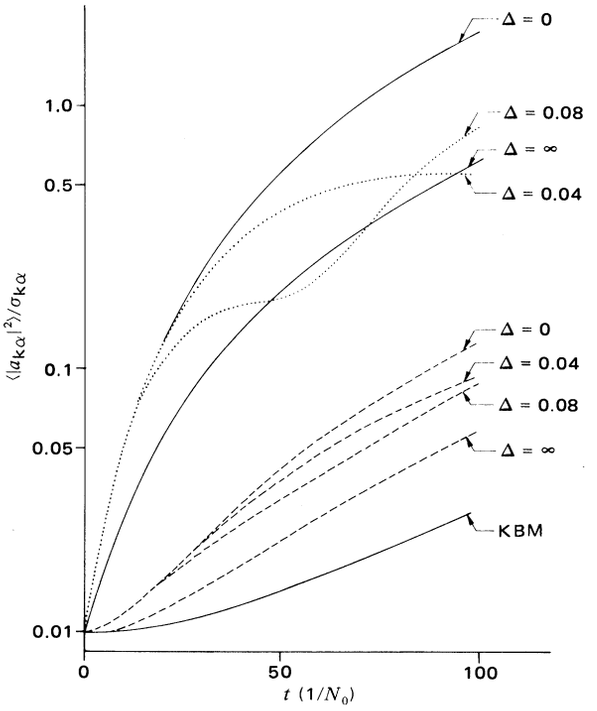

FIG. 2. Mean test wave action for the two-row model. The ambient initial phases are fixed to give maximal initial growth rates for the upper four curves and chosen randomly for the dashed curves. The KBM curve is given by the random phase approximation.

initial conditions results in "square wave" phase oscillations and maximum coupling of the interacting waves (12). These coherent solutions show that the effect of off-resonant triads is to produce oscillations about the growth rates of the resonant triads. For $t \ll 1/\Delta_{max}$ the growth rate is essentially given by the $\Delta_{max} = 0$ curve. For later times the action oscillates about the $\Delta_{max} = \infty$ curve (where in effect only 13 resonant triads are kept, all with $\Delta = 0$). The frequency of these oscillations depends linearly on Δ_{max}.

For the dashed curves in Fig. 2 the initial phases are chosen randomly. From Eqs. **3.1** we see that the initial growth rate of the mean action is zero. For later times, the growth rate (calculated as an average over 100 ambient initial conditions) is about half of the maximal rate. As Δ_{max} is increased, the growth rate decreases as before, but now the oscillations are washed out by the phase averages. The ambient phases do not, however, remain completely random for $t > 0$ because the random phase approximation with the KBM perturbation method (13) yields the lowest curve in Fig. 2. The KBM and maximal rates represent extremes, the first implying complete incoherence while the latter implies complete coherence.

As a final model, more closely related to the full ocean calculation, we include only triads on a single resonance curve, again setting the Gs equal. With this model we can discuss the effect of both Δk and Δ_{max} on the growth rate. As predicted by a Langevin description, we tentatively assume that the test wave relaxes exponentially to equilibrium. To provide a rough estimate for the growth rate, ν, we calculate the time, $t_{1/2}$, required for the test wave to grow to half of its equilibrium value. Then $\nu = -\log 2/t_{1/2}$. The exponential relaxation assumption is clearly not valid for very short times when $\langle|a_{k\alpha}|^2\rangle$ grows as t^2 (because the ambient phases are initially random). For longer times the oscillations caused by nonresonant triads must also provide an error in the fit. However for the purpose of investigating the effects of changing Δk and Δ_{max} our measure is sufficient.

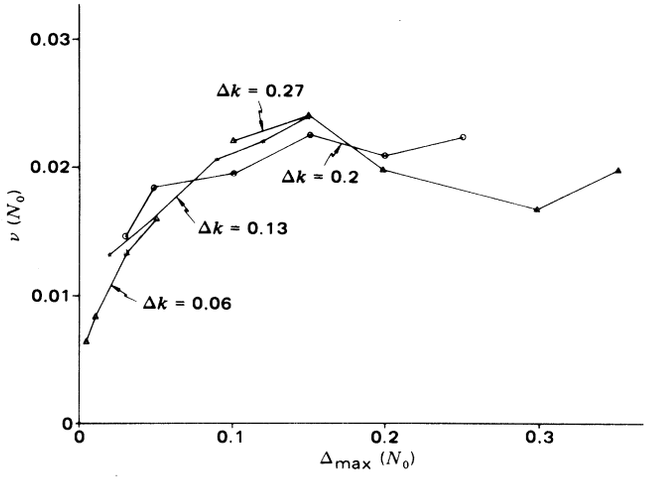

FIG. 3. Growth rate, ν, as a function of Δ_{max} and Δk for the single resonance curve model.

In Fig. 3 we plot ν as a function of Δ_{max} for various values of Δk. These curves approach $\nu \approx 0.02\ N_0$ for $\Delta_{max} \gtrsim 0.1\ N_0$ independently of Δk. Because varying Δk changes the number of triads within a given resonance width, we see that keeping a small number of triads is sufficient to obtain a good estimate of ν. For example, the value of ν for $\Delta_{max} = 0.1$ and $\Delta k = 0.27$ (14 triads) differs by only 15% from that with $\Delta k = 0.10$ (93 triads). Varying the initial action between $10^{-4}\ \sigma_{k\alpha}$ and $0.05\sigma_{k\alpha}$ does not significantly change the growth rate. Further increase of the initial action changes the growth rates drastically, indicating that the exponential assumption breaks down.

Because Δ_{max} and ν define the only available time scales, these quantities can be expected to scale together and produce reliable results if Δ_{max} is chosen self-consistently to be "a few times ν."

Finally, in Fig. 4 we see that the time required for the test

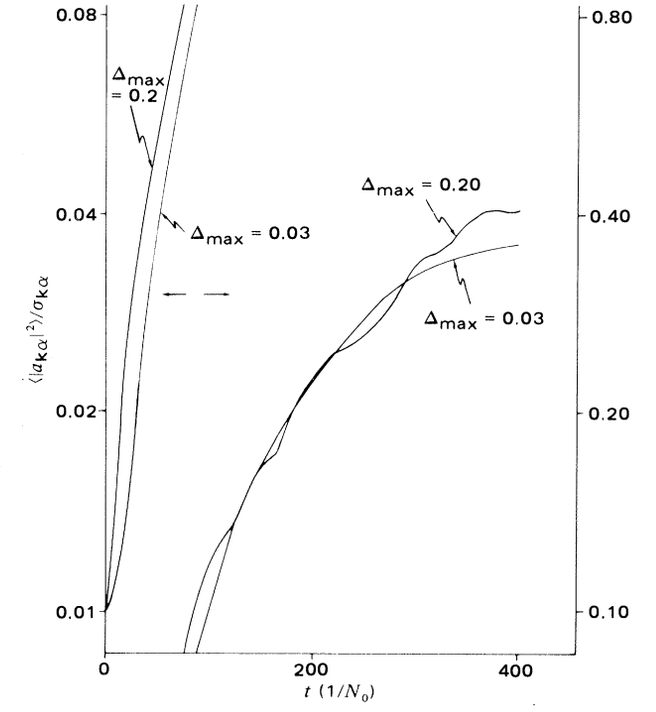

FIG. 4. Mean test wave action for the single resonance model. For $t \lesssim 100/N_0$ the $\Delta_{max} = 0.20$ solution grows faster than the $\Delta_{max} = 0.03$ solution. For longer times (right scale and right curves) evolution is at similar rates.

wave action to reach equilibrium does not depend strongly on Δ_{max}. Although initially the two curves grow at quite different rates [$\nu(\Delta_{max} = 0.03\, N_0) \approx 1.5\, \nu(\Delta_{max} = 0.2\, N_0)$], for later times the curves grow at similar rates and reach their equilibrium values at comparable times.

Appendix

The coupling coefficients that appear in Eqs. **2.19** and **2.23** of the main text are defined explicitly by the following set of equations:

$$\Gamma_2 = \rho_0(32\omega_\alpha\omega_\beta\omega_\gamma e_{k\alpha}e_{l\beta}e_{m\gamma})^{-1/2}[\mathcal{G}(k;l,m) + \mathcal{G}(l;m,k) + \mathcal{G}(m;k,l)]/3, \quad [\mathbf{A.1}]$$

$$\mathcal{G}(k;l,m) = (\omega_\beta^2 - \omega_\gamma^2)\,\mathbf{l}\times\mathbf{m}\cdot\frac{\mathbf{f}}{\omega_\alpha}\left(\frac{\mu^k_{lm}}{k^2} - \frac{\nu_{klm}}{k^2l^2m^2}(\mathbf{l}\cdot\mathbf{m})\right) + i(\omega_\alpha^2 - f^2)\left[\left(\frac{\mu^l_{km}}{l^2} + \frac{\mu^m_{kl}}{m^2}\right)(\mathbf{l}\cdot\mathbf{m}) + \frac{\nu_{klm}}{k^2l^2m^2}\left((\mathbf{l}\cdot\mathbf{k})(\mathbf{k}\cdot\mathbf{m}) + (\mathbf{l}\times\mathbf{m})^2\frac{f^2}{\omega_\beta\omega_\gamma}\right)\right], \quad [\mathbf{A.2}]$$

$$\Gamma_1(\mathbf{k},\omega_\alpha;\mathbf{l},\omega_\beta,\mathbf{m},\omega_\gamma) = 3\Gamma_2(\mathbf{k},\omega_\alpha,-\mathbf{l},-\omega_\beta,-\mathbf{m},-\omega_\gamma), \quad [\mathbf{A.3}]$$

$$\mu^k_{lm} \equiv \frac{1}{\rho_0}\int_{-H}^{0} dz\ \rho\, W'_{k\alpha}W_{l\beta}W_{m\gamma}, \qquad \nu_{klm} \equiv \frac{1}{\rho_0}\int_{-H}^{0} dz\ \rho\, W'_{k\alpha}W'_{l\beta}W'_{m\gamma}, \quad [\mathbf{A.4}]$$

$$G^{kl}_m = -i\frac{k}{lm}\sqrt{\frac{2\omega_\beta\omega_\gamma e_{l\beta}e_{m\gamma}}{\omega_\alpha e_{k\alpha}}}\,B^{1/2}N_0\,\Gamma_1^*(m;k,l). \quad [\mathbf{A.5}]$$

$$G^{k}_{lm} = -\frac{i}{2}\frac{k}{lm}\sqrt{\frac{2\omega_\beta\omega_\gamma e_{l\beta}e_{m\gamma}}{\omega_\alpha e_{k\alpha}}}\,B^{1/2}N_0\,\Gamma_1(k;l,m). \quad [\mathbf{A.6}]$$

The authors express appreciation to Lawrence Berkeley Laboratory for the use of its computing facilities and to N. Pereira and P. Yau for helpful discussions. This research was partially supported by the Office of Naval Research under Contract N00014-78-C-0050.

1. Phillips, O. M. (1977) *The Dynamics of the Upper Ocean* (Cambridge Univ. Press, New York).
2. Davidson, R. C. (1972) *Methods in Nonlinear Plasma Theory* (Academic, New York), pp. 133–173.
3. Jorna, S., ed. (1978) *Topics in Nonlinear Dynamics*, American Institute of Physics Conference Proceedings No. 46 (American Institute of Physics, New York).
4. Hasselmann, K. (1966) *Rev. Geophys.* **4,** 1–32.
5. Snider, R. F. (1960) *J. Chem. Phys.* **32,** 1051–1060.
6. Brout, R. & Prigogine, I. (1956) *Physica* **22,** 621–636.
7. McComas, C. H. & Bretherton, F. P. (1977) *J. Geophys. Res.* **82,** 1397–1412.
8. Olbers, D. J. (1976) *J. Fluid Mech.* **74,** 375–399.
9. Bretherton, F. P. & Garrett, C. J. R. (1969) *Proc. R. Soc. London Ser. A* **302,** 529–554.
10. Meiss, J. D. & Watson, K. M. (1978) in *Topics in Nonlinear Dynamics*, ed. Jorna, S. (American Institute of Physics, New York), pp. 296–323.
11. Garrett, C. J. R. & Munk, W. H. (1975) *J. Geophys. Res.* **80,** 291–297.
12. Meiss, J. D. (1979) *Phys. Rev. A*, in press.
13. Bogoliubov, N. N. & Mitropolsky, Y. A. (1961) *Asymptotic Methods in the Theory of Nonlinear Oscillations* (Gordon & Breach, New York).